



BIOMECHANICAL REPORT

FOR THE

IAAF World Championships
LONDON 2017

High Jump Men's

Dr Gareth Nicholson and Dr Athanassios Bissas
Carnegie School of Sport

Stéphane Merlino
IAAF Project Leader



LEEDS
BECKETT
UNIVERSITY

IAAFTM

Event Director
Dr Gareth Nicholson

Project Director
Dr Athanassios Bissas

Project Coordinator
Louise Sutton

Senior Technical Support

Liam Gallagher

Aaron Thomas

Liam Thomas

Senior Research Officer
Josh Walker

Report Editor
Dr Catherine Tucker

Analysis Support
Dr Lysander Pollitt

Logistics
Dr Zoe Rutherford

Calibration
Dr Brian Hanley

Data Management
Nils Jongerius

Ashley Grindrod
Joshua Rowe

Technical Support
Ruth O'Faolain

Lewis Lawton
Joe Sails

Data Analysts

Dr Gareth Nicholson

Emily Gregg

Nils Jongerius

Project Team

Dr Tim Bennett

Mark Cooke
Helen Gravestock

Dr Alex Dinsdale

Masalela Gaesenngwe

Mike Hopkinson

Parag Parelkar

Rachael Bradley
Jamie French
Philip McMorris
William Shaw
Dr Emily Williams

Amy Brightmore
Callum Guest
Maria van Mierlo
James Webber
Jessica Wilson
Dr Stephen Zwolinsky

Helen Davey
Ruan Jones
Dr Ian Richards
Jack Whiteside
Lara Wilson

External Coaching Consultant
Denis Doyle

Table of Contents

INTRODUCTION	1
METHODS	2
RESULTS	7
COACH'S COMMENTARY	26
CONTRIBUTORS	30

Figures

Figure 1. Camera locations for the men's high jump final (highlighted in green).	2
Figure 2. The calibration frame was constructed and filmed before and after the competition.	3
Figure 3. Action from the men's high jump final.	4
Figure 4. Key time-points at which the selected variables were obtained. C1-C4 denote foot contacts.	4
Figure 5. Partial heights of each athlete's CM during their best attempt.	7
Figure 6. Scatterplot showing the distance of the CM (peak height) relative to the cleared mark in the vertical and horizontal directions for each finalist. Minus value on the horizontal scale indicate area beyond the bar.	8
Figure 7. Contrasting bar clearance techniques of the medallists, with Barshim (top), Lysenko (middle) and Ghazal (bottom).	9
Figure 8. Mean height (% of each athlete's stature) of the CM during each foot contact throughout the approach (before commencement of the take-off phase).	11
Figure 9. The vertical position of the CM during the approach for the gold medallist.	11
Figure 10. Horizontal velocity of the centre of mass at TD during the second, third and fourth (take-off) foot contacts.	12
Figure 11. Contrasting rear foot position during take-off TD for three of the finalists.	13
Figure 12. Overhead view of the CM path during the approach, take-off and airborne phase. Dashed lines depict the construction of the CM attack angles reported in Table 6.	14
Figure 13. Schematic representation of the step-to-bar angle for each foot contact relative to the next.	15
Figure 14. The overhead views of the paths of the CM during the approach and take-off for the finalists. Medallists are represented by solid lines.	16
Figure 15. Overhead views of the CM and foot path during the approach, take-off and airborne phases for the three medallists.	17
Figure 16. Length of the last three approach steps for each of the finalists.	18

Figure 17. The contrasting take-off distances of Lysenko (left) and Bondarenko (right).	19
Figure 18. Scatterplots showing the relationships between key variables. r values indicate correlation coefficients.	20
Figure 19. The range of motion of the knee (take-off leg) between maximum flexion and take-off for each of the finalists. The medallists have been highlighted in their respective medial colours whilst the remaining finalists are displayed in black.	21
Figure 20. Top: Contact times for the final four ground contacts during the approach for each of the finalists. Bottom: Flight times for the final three steps before take-off (flight 3 precedes contact 4) for each of the finalists.	22
Figure 21. Top: Ratio of flight time to ground contact time during the final step. Bottom: relationship between the ratio and knee angle at maximum flexion during the take-off phase.	23
Figure 22. The percentage of time spent during knee flexion and extension during the final foot contact (take-off phase).	24
Figure 23. Example of body orientation at TD during the take-off phase for Barshim.	25

Tables

Table 1. Definitions of mechanical and performance variables.	5
Table 2. Best mark attained for each of the finalists expressed relative to their previous bests (before the London World Championships).	7
Table 3. Partial heights of the CM (in metres and relative to each athlete's stature) along with the peak CM location, peak pelvis height and PPH diff for each finalist.	8
Table 4. The height (relative to stature) of the CM at contact two, three and four along with the change in height (% of stature) during the take-off phase, mean approach height (% stature) and the percentage lowering of the CM from penultimate to final TD (not relative to stature).	10
Table 5. The horizontal velocity of the CM at TD during each foot contact (fourth contact = take-off) and at TO of contact four. The change (%) in horizontal velocity during take-off (from TD to TO) is also displayed.	12
Table 6. CM attack angle at toe-off for the first, second, third and fourth foot contacts along with the percentage change in this angle from the first to the fourth foot contact.	14
Table 7. Step-to-bar angle between toe-off to toe-off of each respective foot contact along with the percentage change in these angles from one to the next (1-3 indicates the % change from the first to the final angle).	15
Table 8. The length of the last three approach steps along with the contact time of the take-off phase (CT) for the finalists. Step lengths are also expressed as a percentage of each athlete's standing height.	18
Table 9. The vertical (V_v) and resultant (V_r) velocity values at TD and TO during the take-off phase along with the velocity transfer, take-off angle and take-off distances.	19
Table 10. The knee angles at the instant of touchdown (TD) and toe-off (TO) during the penultimate foot contact for all finalists. Knee and ankle angles are also displayed at TD, TO and its lowest value during the final (take-off) contact.	21
Table 11. The time spent in knee flexion and extension during the penultimate and final foot contacts.	24
Table 12. The whole-body lean at touchdown and toe-off during the take-off phase and the trunk lean at touchdown for each of the finalists.	25

INTRODUCTION

The men's high jump final took place on the night of August 13th in good weather conditions. Approaching the event, the overriding favourite was Mutaz Essa Barshim with the Qatari remaining undefeated in his last six competitions and topping the outdoor season's best list with a mark of 2.38 m. Despite favourable conditions, none of the finalists surpassed their season's best. On the night, Barshim lived up to expectations surpassing his silver medal in the same stadium in 2012 and his disappointing fourth place finish in the last World Championships. The 26 year-old produced an impressive score card clearing 2.20 m, 2.25 m, 2.29 m, 2.32 m and 2.35 m. Despite holding the Asian record from 2014 with a mark of 2.43 m, Barshim was unable to raise the world lead to 2.40 m during his final attempts. Although it was Germany's Mateusz Przybylko who had come closest to Barshim's world lead in 2017, it was Daniel Lyenko and Majd Eddin Ghazal who took silver and bronze respectively, with Lyenko competing through lingering pain caused by a recent injury to his take-off leg.

IAAF World Championships		London 4-13 August 2017		IAAF World Championships LONDON 2017											
RESULTS															
High Jump Men - Final															
RECORDS World Record WR 2.45 Javier SOTOMAYOR CUB 26 Salamanca (Helmántico) 27 Jul 1993 Championships Record CR 2.41 Bohdan BONDARENKO UKR 24 Moskva (Luzhniki) 15 Aug 2013 World Leading WL 2.38 Mutaz Essa BARSHIM QAT 26 Oslo (Bislett) 15 Jun 2017 Area Record AR National Record NR Personal Best PB Season Best SB															
13 August 2017 19:00 START TIME		22° C TEMPERATURE		35 % HUMIDITY											
20:38 END TIME		22° C		35 %											
PLACE	NAME	COUNTRY	DATE OF BIRTH	ORDER	RESULT	2.20	2.25	2.29	2.32	2.35	2.40				
1	Mutaz Essa BARSHIM	QAT	24 Jun 91	3	2.35	0	0	0	0	0	XXX				
2	Danil LYSENKO	ANA	19 May 97	6	2.32	0	0	X0	0	XXX					
3	Majd Eddin GHAZAL	SYR	21 Apr 87	11	2.29	0	0	X0	XXX						
4	Edgar RIVERA	MEX	13 Feb 91	12	2.29	0	0	XX0	XXX						
5	Mateusz PRZYBYLKO	GER	9 Mar 92	1	2.29	0	X0	XX0	XXX						
6	Robert GRABARZ	GBR	3 Oct 87	9	2.25	0	0	XXX							
6	Ilya IVANYUK	ANA	9 Mar 93	5	2.25	0	0	XXX							
8	Bryan MCBRIDE	USA	10 Dec 91	4	2.25	0	X0	XXX							
9	Bohdan BONDARENKO	UKR	30 Aug 89	10	2.25	-	XX0	-	XXX						
10	Eike ONNEN	GER	3 Aug 82	7	2.20	XX0	XXX								
	Tihomir IVANOV	BUL	11 Jul 94	8	NM	Xr									
	Yu WANG	CHN	18 Aug 91	2	DNS										
Timing and Measurement by SEIKO						AT-HJ-M-f--A--RS1..v1						Issued at 20:40 on Sunday, 13 August 2017			
Official Partners															
TDK		TOYOTA		asics		SEIKO		EUROVISION		TBS					

METHODS

Unlike the qualification rounds, the landing mat for the high jump finals was positioned centrally (with respect to the field inside the running track) at the north side of the stadium. Four vantage locations for camera placement were identified and secured with each location having the capacity to accommodate at least one camera mounted on a tripod. Three of the locations were located on the north side of the stadium on broadcasting platforms whilst the remaining location was situated on the broadcasting balcony at the start of the home straight.

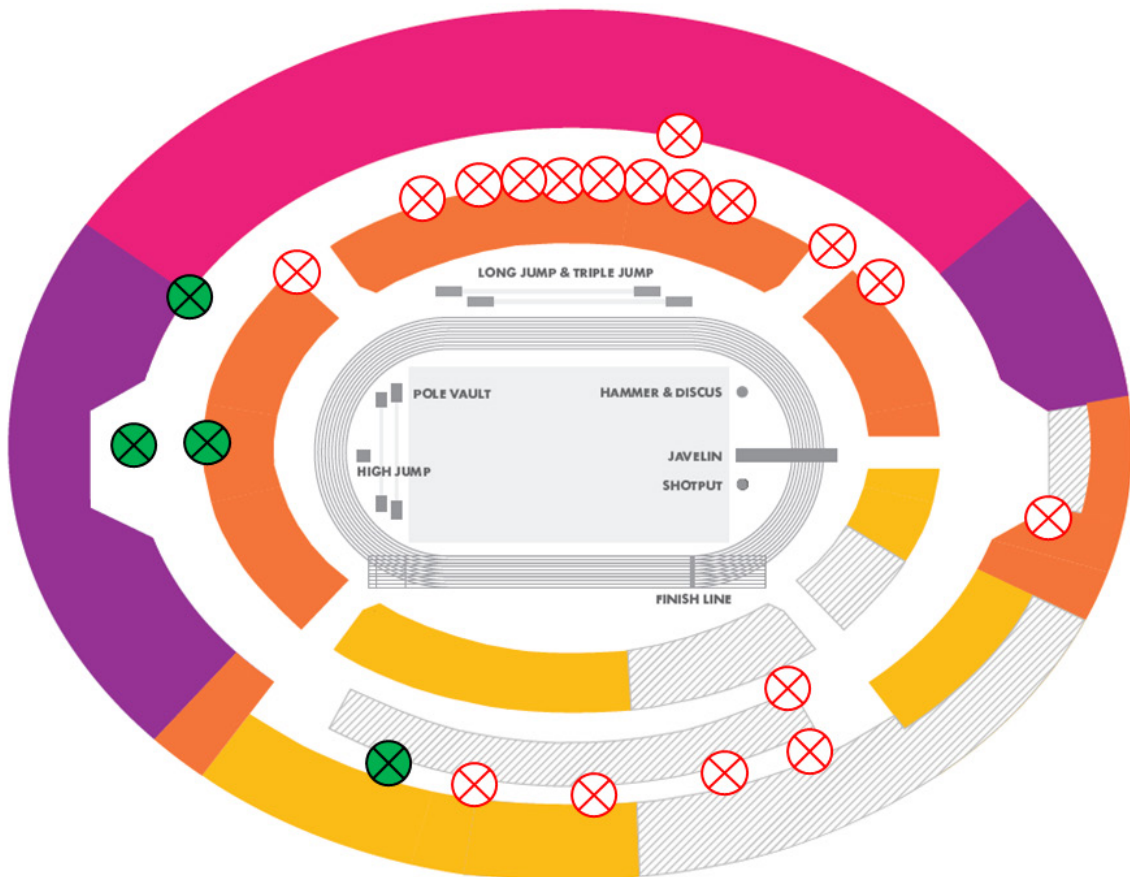


Figure 1. Camera locations for the men's high jump final (highlighted in green).

One standardised calibration procedure was conducted before and after the commencement of events on the evening of the final. Specifically, a rigid cuboid calibration frame was filmed on the high jump run-up / take-off area and repositioned multiple times over discrete predefined areas. This ensured an accurate defined volume for athletes who approached the uprights from both left and right directions. This approach produced a large number of non-coplanar control points per individual calibrated volume and facilitated the construction of a three-dimensional global coordinate system.

A total of five high-speed cameras were employed to record the action during the men's high jump final. Sony RX10 M3 cameras operating at 120 Hz (shutter speed: 1/1600; ISO: 1600; FHD: 1920x1080 px) were positioned strategically in pairs with their optical axes positioned to capture each athlete's attempt in both the frontal and sagittal planes. Separate camera pairings were utilised for athletes with left- and right-footed take-offs which enabled full-body motion capture to take place commencing three steps before take-off and ending when the athlete had landed.



Figure 2. The calibration frame was constructed and filmed before and after the competition.

The video files were imported into SIMI Motion (SIMI Motion version 9.2.2, Simi Reality Motion Systems GmbH, Germany) and the highest successful attempt for each athlete was manually digitised by a single experienced operator to obtain kinematic data. An event synchronisation technique (synchronisation of four critical instants) was applied through SIMI Motion to synchronise the two-dimensional coordinates from each camera involved in the recording. Digitising started 15 frames before the beginning of the first touchdown and ended 15 frames after the required sequence to provide padding during filtering. Each file was first digitised frame by frame and upon completion adjustments were made as necessary using the points over frame method, where each point (e.g. right knee joint) was tracked through the entire sequence. The Direct Linear Transformation (DLT) algorithm was used to reconstruct the real-world 3D coordinates from individual camera's x and y image coordinates. Reliability of the digitising process was estimated by repeated digitising of one full trial with an intervening period of 48 hours. The results showed minimal systematic and random errors and therefore confirmed the high reliability of the digitising process. De Leva's (1996) body segment parameter models were used to obtain data for the whole body centre of mass and for key body segments. A recursive second-order, low-pass Butterworth digital filter (zero phase-lag) was employed to filter the raw coordinate data. The cut-off frequencies were calculated using residual analysis. Where available,

athletes' heights were obtained from 'Athletics 2017' (edited by Peter Matthews and published by the Association of Track and Field Statisticians) and online sources.



Figure 3. Action from the men's high jump final.

Each athlete's attempt was split into three consecutive parts:

1. *The Approach*: from the instant at which the athlete begins approaching the bar until the instant of touch-down for the take-off.
2. *The Take-off*: from the instant of touch-down (in the final contact) until the instant at which the take-off foot ends contact with the ground.
3. *The Flight/Bar Clearance*: from the instant of take-off until the instant of landing.

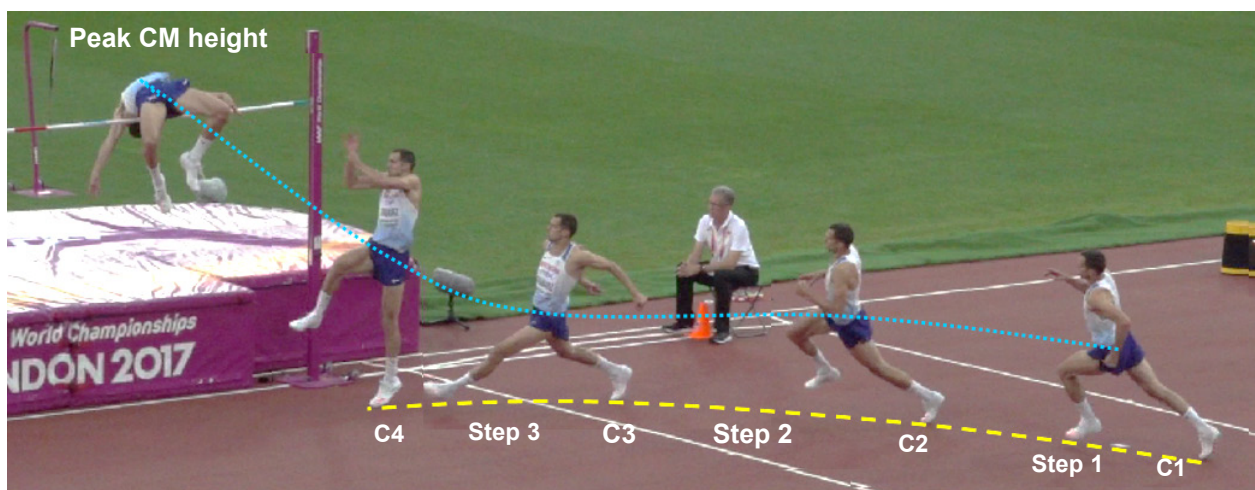


Figure 4. Key time-points at which the selected variables were obtained. C1-C4 denote foot contacts.

As the take-off conditions depend on the characteristics of the approach steps, the support and flight times, step lengths, centre of mass (CM) height, path of the centre of mass, angle of the run-up and horizontal / vertical velocities were computed throughout the last three steps of the athletes run-up. With regards to take-off, the contact time, distance from the bar, body segment angles, take-off angle, horizontal/vertical velocities and location of the CM were computed (in some instances certain values could not be computed for certain athletes because of the mat being moved immediately before the commencement of the final). To complete the analysis, the peak height of the CM and location of the peak CM height with respect to the bar was obtained. In addition to an in-depth understanding of the characteristics of each finalist's best jump, the aforementioned parameters enabled the attempts to split into the following three partial heights:

1. *H1*: the height of the CM at the instant of touch-down (TD) during the final contact.
2. *H2*: the height of the CM at the instant of toe-off (TO) during the take-off phase.
3. *H3*: the peak vertical height of the CM during flight.

Table 1. Definitions of mechanical and performance variables.

Variable	Definition
CM height	The vertical height of the CM at various instances during the approach, take-off and flight.
Δ TO height (%)	The change in CM height (percentage of standing height) from TD to TO during the take-off phase.
Mean CM height	The mean height (% of standing height) of the CM at TD and TO throughout the approach (not including final TO).
% CM lowering	The percentage difference in CM height at TD between the penultimate and final foot contact.
Peak CM location	The anteroposterior distance of the CM from the bar at the instant of peak CM height.
Peak pelvis height	The maximum vertical height of the pelvis during flight.
PPH diff	The difference between peak pelvis height and the mark attained.
Path of run-up	The overhead representation of the path of the CM during the last three approach steps.
CM attack angle at TO 1-4	The angle between the peak CM position over the bar and the CM position at toe-off of each foot contact during the run-up (viewed overhead).
Step to bar angle at foot contacts 1-3	The angle between each respective foot contact relative to the bar.

Take-off distance (TOD)	The foot-tip distance (anteroposterior) from the bar at take-off.
Step length (SL)	The displacement between toe-off of consecutive foot contacts.
Contact time (CT)	The time spent in contact with the ground during each foot contact.
Flight time (FT)	The time spent airborne during each step of the approach.
Ratio (FT/CT)	The flight time divided by the subsequent contact time.
Vertical velocity (V_v)	The vertical velocity of the CM at various time instants.
Horizontal velocity (V_h)	The horizontal velocity (resultant of anteroposterior and mediolateral components) of the CM at various time instants.
Resultant velocity (V_r)	The resultant velocity of the CM at various time instants.
Ratio of velocity change ($\Delta V_v / \Delta V_h$)	The change in vertical velocity relative to the change in horizontal velocity during the take-off phase.
Velocity transfer	The change in vertical velocity (from TD to TO) relative to the horizontal velocity at TD during the take-off phase.
Take-off angle	The angle of the CM relative to the horizontal at the instant of take-off (calculated from take-off velocities).
Knee angle at TD/TO	The angle of the thigh relative to the shank at the instant of TD / TO during the penultimate or final foot contact. (180° = full extension)
Knee / Ankle lowest	The minimum angle of the knee and ankle during the take-off phase.
Ankle angle at TD/TO	The angle of the shank relative to the foot at the instant of TD / TO during take-off. (180° = full plantar flexion)
Knee flexion / extension duration	The time between maximum knee flexion and TD or TO during take-off.
Whole-body lean at TD/TO	The angle of the line between the CM and ankle joint (take-off leg) relative to the vertical at TD and TO during the take-off phase.
Trunk lean at TD	The angle of the trunk relative to the vertical at TD during the take-off phase.
Side-ways trunk lean at TD	The lean angle of the trunk (inward / outward) relative to the vertical at TD during the take-off phase. Positive values indicate inward lean.

Note: CM = centre of mass.

RESULTS

Table 2 below shows the highest clearance mark for each of the finalists and compares the mark to the season (2017) and personal best for each athlete.

Table 2. Best mark attained for each of the finalists expressed relative to their previous bests (before the London World Championships).

Athlete	Season's best (SB) (m)	Personal best (m)	Mark (m)	Difference from SB (%)
BARSHIM	2.38	2.43	2.35	-1.26
LYSENKO	2.34	2.34	2.32	-0.85
GHAZAL	2.32	2.36	2.29	-1.29
RIVERA	2.30	2.30	2.29	-0.43
PRZYBYLKO	2.35	2.35	2.29	-2.55
GRABARZ	2.31	2.37	2.25	-2.60
IVANYUK	2.31	2.31	2.25	-2.60
MCBRIDE	2.30	2.30	2.25	-2.17
BONDARENKO	2.32	2.42	2.25	-3.02
ONNEN	2.30	2.34	2.20	-4.35

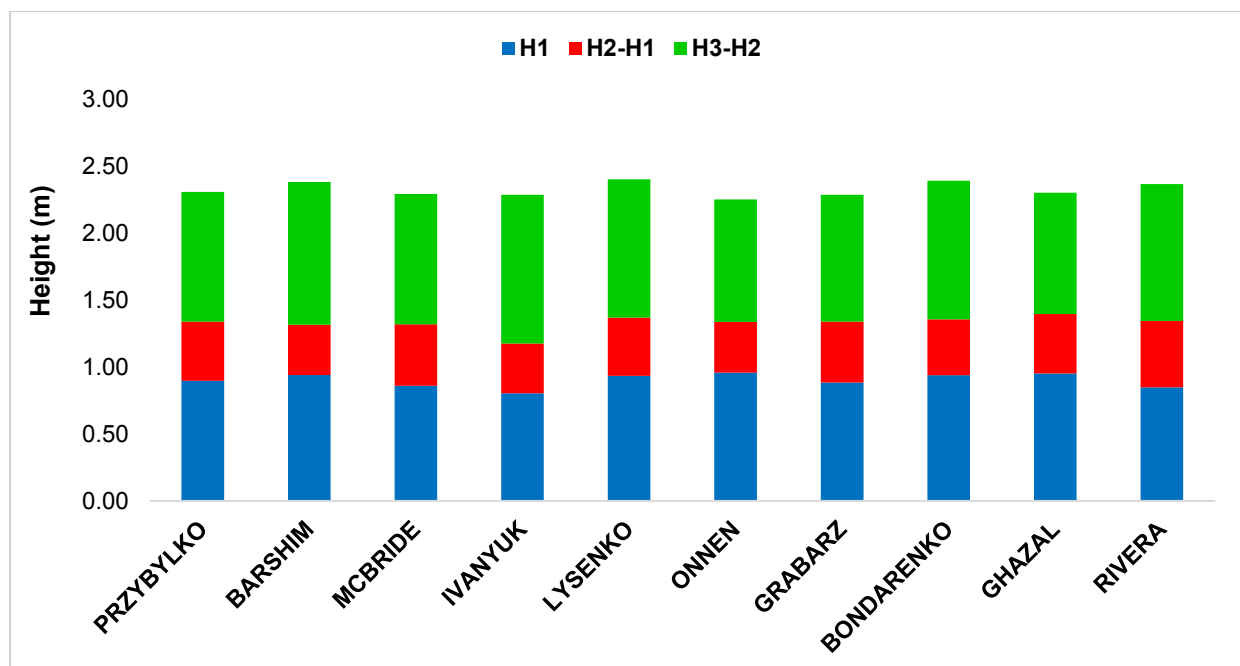


Figure 5. Partial heights of each athlete's CM during their best attempt.

Figure 5 on the previous page shows the partial heights of the CM during the take-off and flight phases of the jumps for each athlete. Table 3 below shows the individual and mean partial heights and also expresses these as a percentage of each athlete's standing height.

Table 3. Partial heights of the CM (in metres and relative to each athlete's stature) along with the peak CM location, peak pelvis height and PPH diff for each finalist.

Athlete	H1 (m)	H2 (m)	H3 (m)	H3 diff (m)	H1 (%)	H2 (%)	H3 (%)	Peak CM location (m)	Peak pelvis height (m)	PPH diff (m)
BARSHIM	0.94	1.31	2.38	0.03	48.96	68.44	123.96	0.00	2.52	0.17
LYSENKO	0.93	1.37	2.40	0.08	48.65	71.25	125.00	-0.29	2.49	0.17
GHAZAL	0.95	1.40	2.30	0.01	49.33	72.28	119.17	-0.08	2.42	0.13
RIVERA	0.85	1.34	2.37	0.08	44.40	70.31	123.82	0.23	2.47	0.18
PRZYBYLKO	0.90	1.34	2.31	0.02	46.24	68.97	118.87	-0.05	2.46	0.17
GRABARZ	0.88	1.34	2.29	0.04	45.99	69.69	119.01	0.13	2.42	0.17
IVANYUK	0.80	1.18	2.28	0.03	43.88	64.21	124.81	-0.10	2.38	0.16
MCBRIDE	0.86	1.32	2.29	0.04	45.74	70.11	121.81	0.03	2.43	0.18
BONDARENKO	0.94	1.36	2.39	0.14	47.61	68.78	121.32	0.01	2.51	0.26
ONNEN	0.96	1.34	2.25	0.07	49.38	68.87	115.98	-0.01	2.38	0.18

Note: Minus values for peak CM location indicate peak CM beyond the bar.

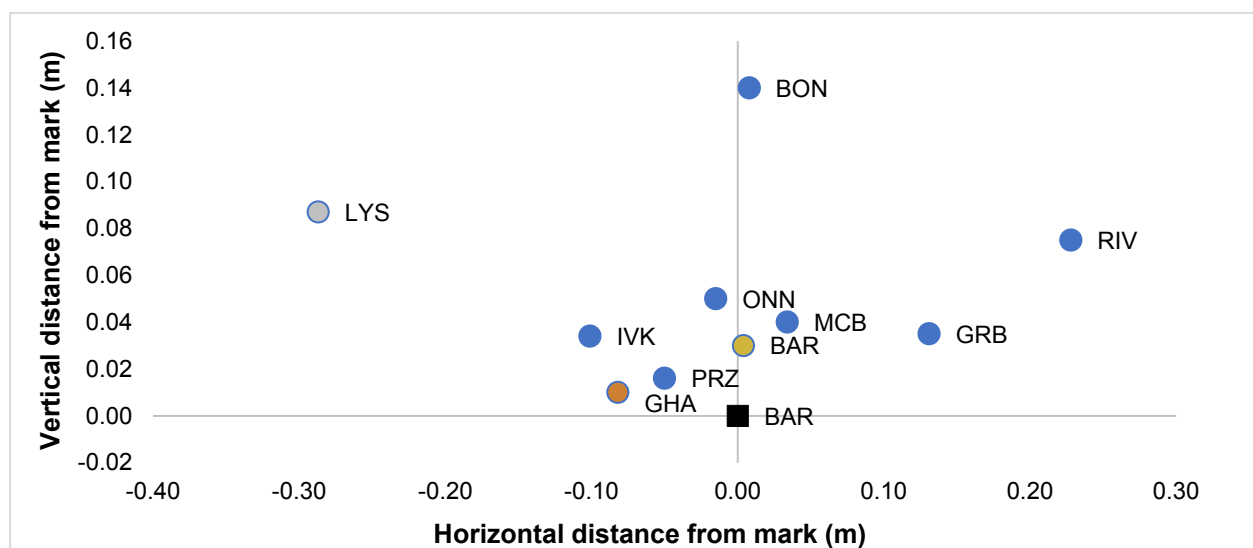


Figure 6. Scatterplot showing the distance of the CM (peak height) relative to the cleared mark in the vertical and horizontal directions for each finalist. Minus value on the horizontal scale indicate area beyond the bar.

Figure 6 on the previous page shows the horizontal and vertical distance of the peak CM height from the bar for each finalist. The contrasting bar clearance techniques of the medallists should be considered when interpreting Figure 6 and Table 3 since this varied between the finalists (Figure 7).

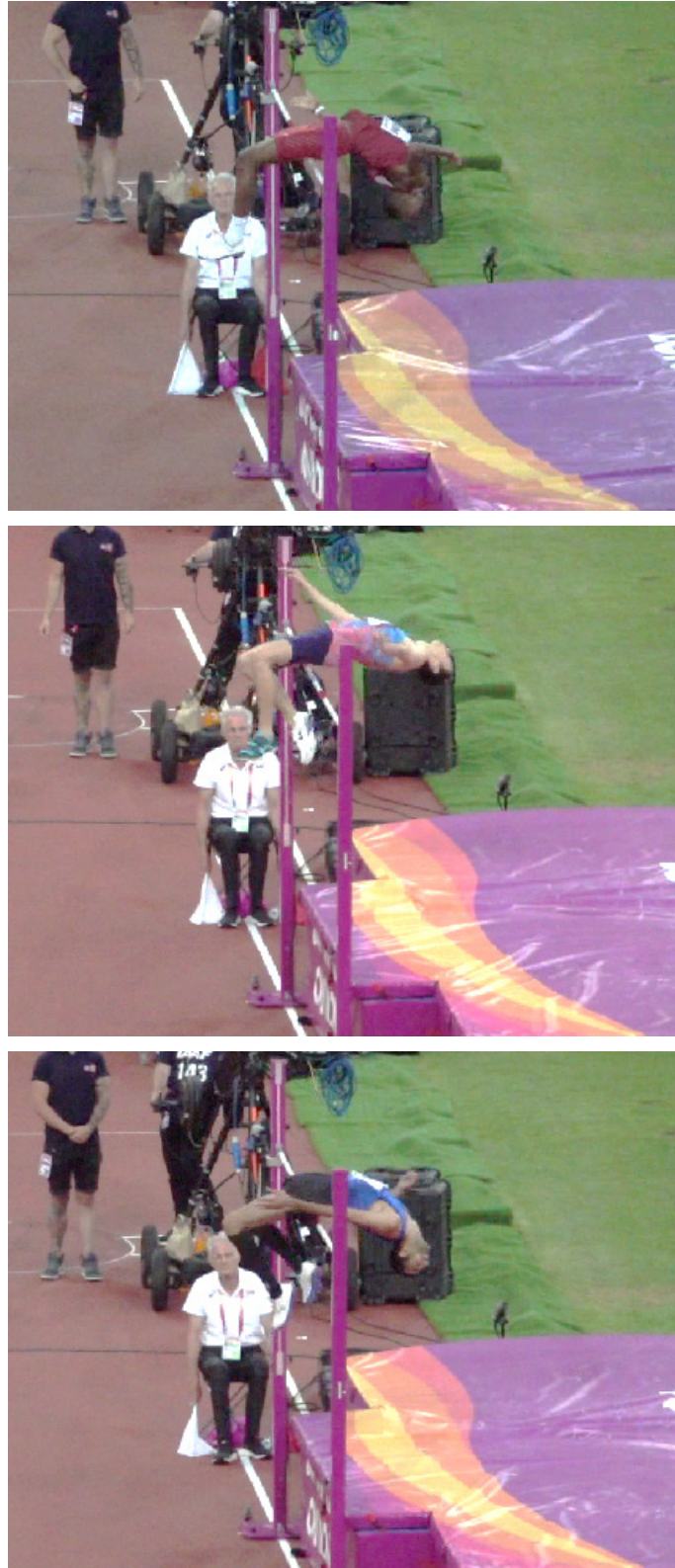


Figure 7. Contrasting bar clearance techniques of the medallists, with Barshim (top), Lysenko (middle) and Ghazal (bottom).

Table 4 below shows the height of the CM at the instant of touchdown during the second, third and fourth foot contacts along with the percentage change in height of the CM during the take-off phase. Table 4 also shows the mean height of the CM during each foot contact during the approach and the percentage lowering of the CM during the last step. Figure 8 on the next page visually depicts the mean CM height for each of the finalists with the medallists being highlighted in their respective colours.

Table 4. The height (relative to stature) of the CM at contact two, three and four along with the change in height (% of stature) during the take-off phase, mean approach height (% stature) and the percentage lowering of the CM from penultimate to final TD (not relative to stature).

Athlete	Contact 2 TD (%)	Contact 3 TD (%)	Contact 4 TD (%)	Mean height (%)	CM lowering (%)	Δ TO height (%)
BARSHIM	51.20	52.29	48.96	51.22	-6.37	19.48
LYSENKO	52.45	51.67	48.65	51.70	-5.85	22.60
GHAZAL	53.16	53.83	49.33	52.72	-8.37	22.95
RIVERA	47.43	47.12	44.40	47.20	-5.78	25.92
PRZYBYLKO	-	46.75	46.24	46.61	-1.10	22.73
GRABARZ	49.53	49.32	45.99	48.84	-6.76	23.70
IVANYUK	46.01	46.01	43.88	45.81	-4.63	20.33
MCBRIDE	45.64	46.76	45.74	46.19	-2.16	24.36
BONDARENKO	47.66	47.36	47.61	47.81	0.54	21.17
ONNEN	50.31	46.86	49.38	49.39	5.39	19.48

Note: Certain values could not be computed for Przybylko.

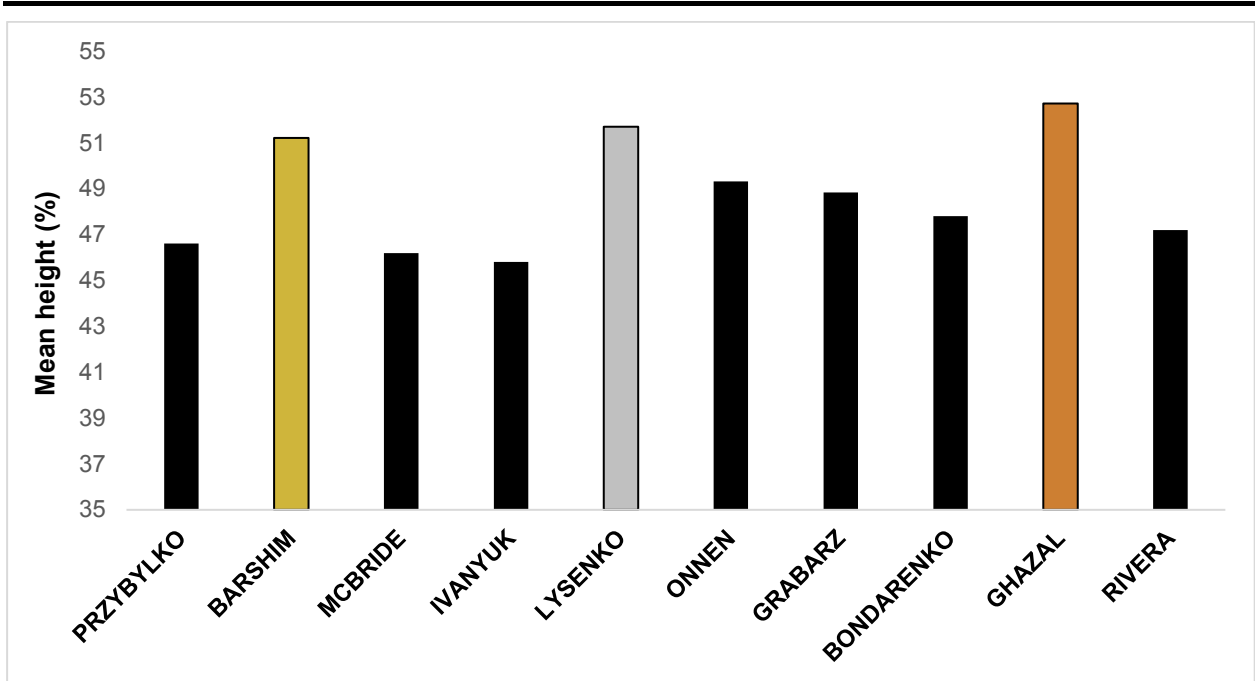


Figure 8. Mean height (% of each athlete’s stature) of the CM during each foot contact throughout the approach (before commencement of the take-off phase).

Figure 9 below shows the vertical position of the CM throughout the approach for the gold medallist.

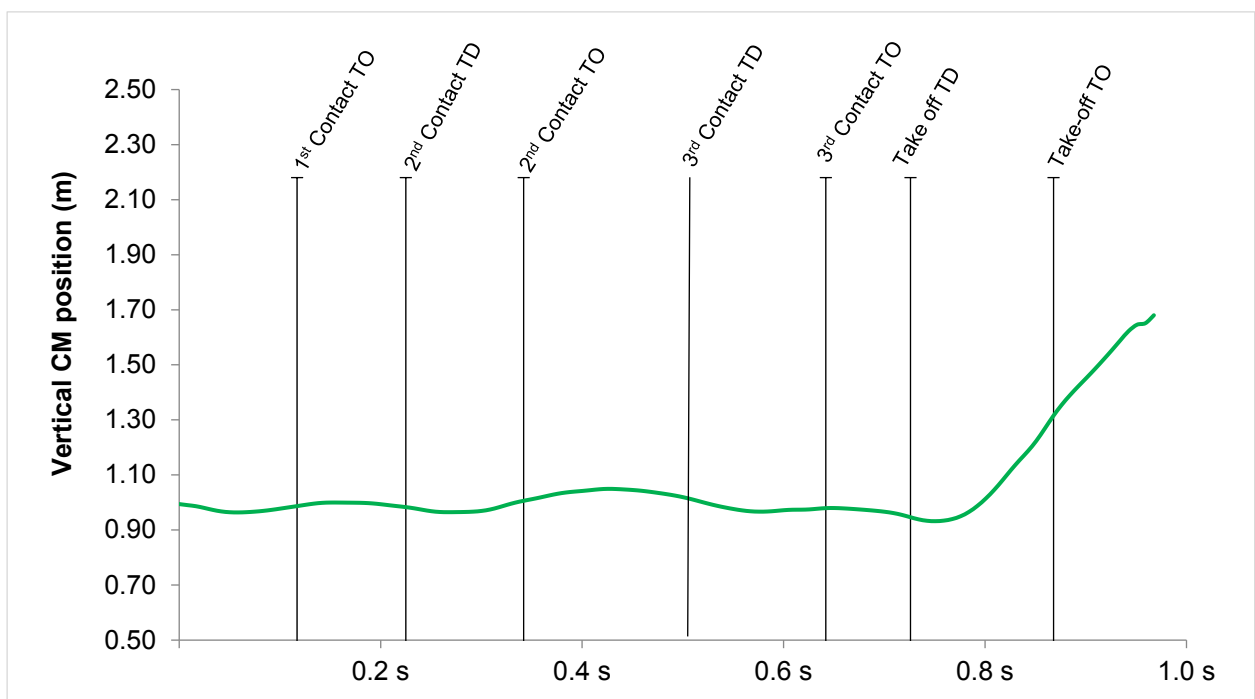


Figure 9. The vertical position of the CM during the approach for the gold medallist.

Table 5 on the next page shows the specific values for the horizontal velocity during each contact as well as the peak velocity during the approach. Figure 10 on the next page shows the horizontal velocity of each finalist during the second, third and fourth foot contacts during the approach.

Table 5. The horizontal velocity of the CM at TD during each foot contact (fourth contact = take-off) and at TO of contact four. The change (%) in horizontal velocity during take-off (from TD to TO) is also displayed.

Athlete	V_h 2 nd contact TD (m/s)	V_h 3 rd contact TD (m/s)	V_h 4 th contact TD (m/s)	V_h 4 th contact TO (m/s)	ΔV_h during take-off (%)
BARSHIM	7.84	7.82	7.46	4.59	-38.47
LYSENKO	7.44	7.23	7.05	3.62	-48.65
GHAZAL	7.30	7.10	7.17	4.03	-43.79
RIVERA	8.01	7.43	7.19	3.51	-51.18
PRZYBYLKO	-	7.79	7.97	4.92	-38.27
GRABARZ	7.73	7.57	7.16	3.84	-46.37
IVANYUK	7.56	7.78	7.06	4.09	-42.07
MCBRIDE	7.77	7.72	7.83	4.13	-47.25
BONDARENKO	6.99	7.83	7.86	4.59	-41.60
ONNEN	7.17	7.29	7.41	4.01	-45.88

Note: Certain values could not be computed for Przybylko.

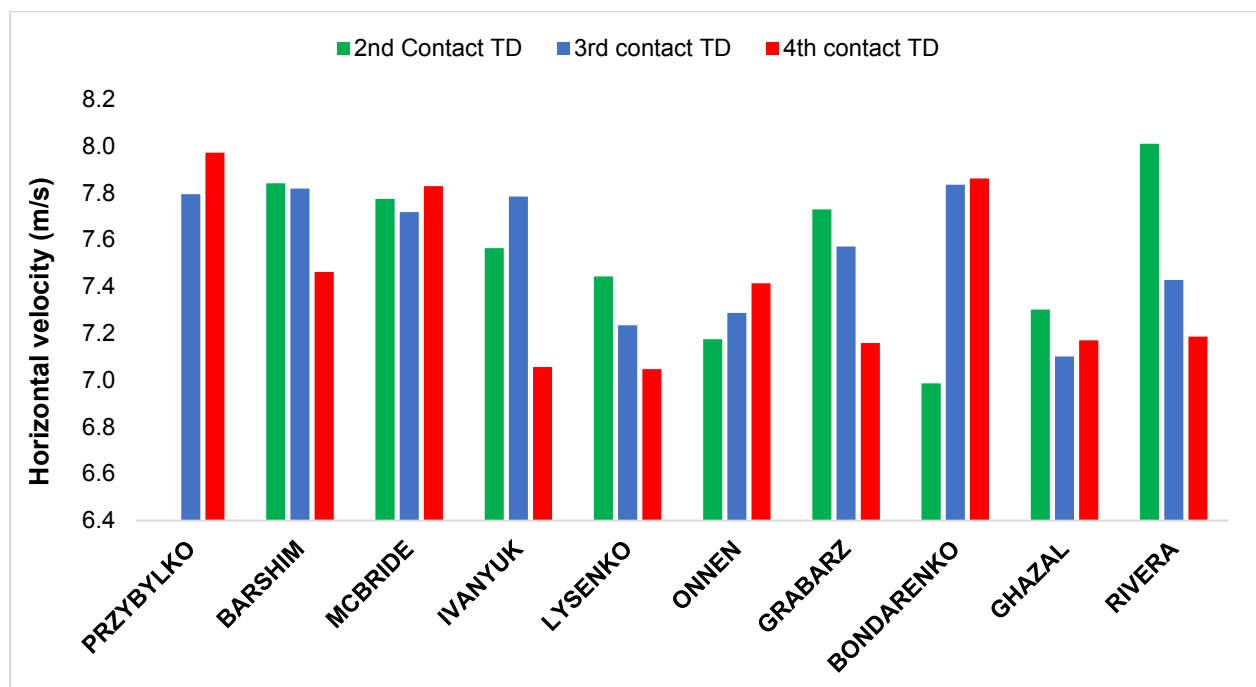


Figure 10. Horizontal velocity of the centre of mass at TD during the second, third and fourth (take-off) foot contacts.

Figure 11 below shows the rear foot position displayed by three of the finalists during the take-off phase.

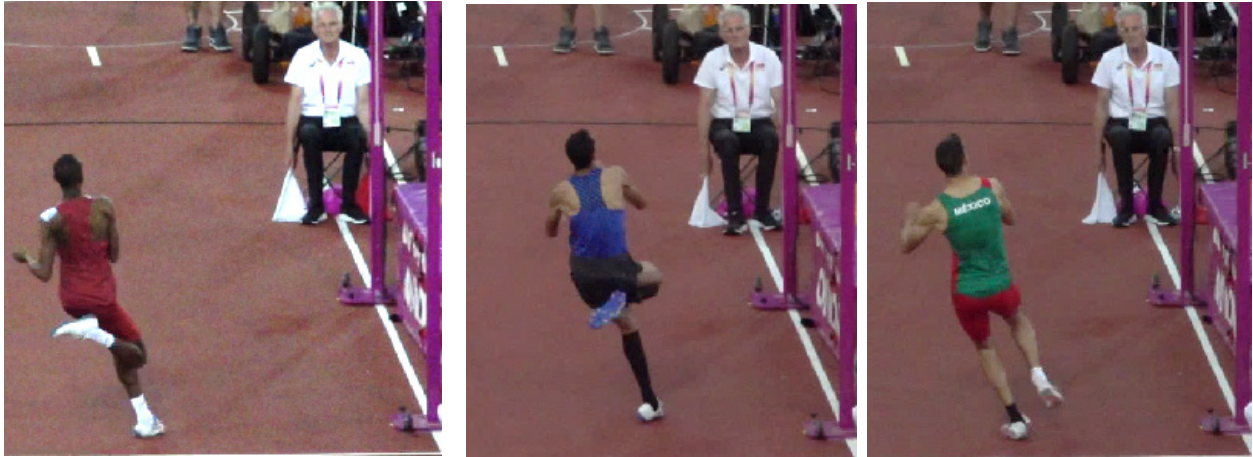


Figure 11. Contrasting rear foot position during take-off TD for three of the finalists.

Table 6 below shows the CM angle of attack at toe-off during the first, second, third and fourth (take-off) foot contacts whilst Figure 12 shows how these angles were constructed. The angles are smaller for athletes who move more parallel to the bar.

Table 6. CM attack angle at toe-off for the first, second, third and fourth foot contacts along with the percentage change in this angle from the first to the fourth foot contact.

Athlete	CM attack angle 1 st TO (°)	CM attack angle 2 nd TO (°)	CM attack angle 3 rd TO (°)	CM attack angle 4 th TO (°)	Δ 4-1 (%)
BARSHIM	58.16	55.72	52.89	52.10	-10.42
LYSENKO	52.92	48.63	46.16	45.03	-14.91
GHAZAL	53.99	51.28	48.08	46.62	-13.65
RIVERA	49.10	45.35	40.69	40.48	-17.56
PRZYBYLKO	-	37.68	33.06	32.58	-
GRABARZ	48.45	43.05	36.94	34.92	-27.93
IVANYUK	44.32	40.62	37.60	36.42	-17.82
MCBRIDE	46.50	43.31	41.56	41.57	-10.60
BONDARENKO	-	49.11	48.19	49.62	-
ONNEN	54.88	47.52	43.57	42.92	-21.79

Note: Certain values could not be computed for Przybylko and Bondarenko.

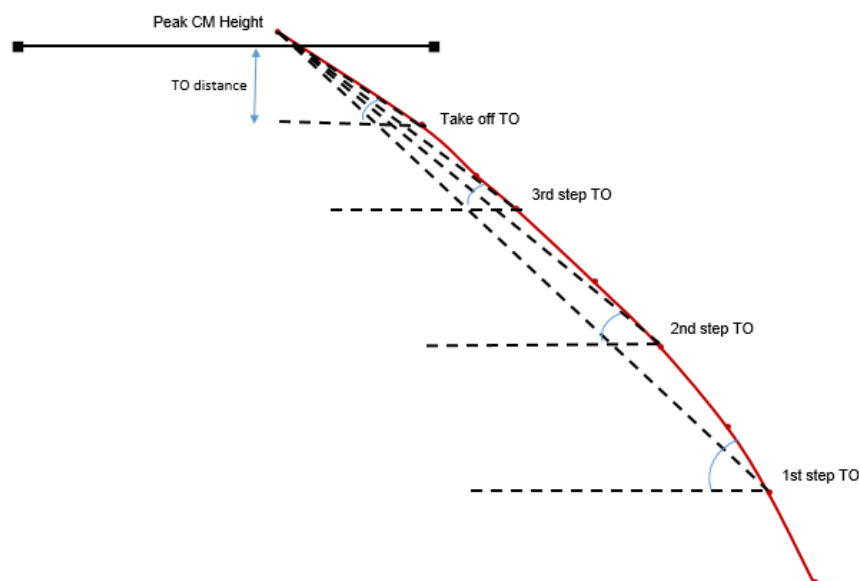


Figure 12. Overhead view of the CM path during the approach, take-off and airborne phase. Dashed lines depict the construction of the CM attack angles reported in Table 6.

Table 7 below shows the step-to-bar angles between each respective foot contact along with the percentage change from each angle to the next. Figure 13 shows how these angles were constructed. The angles are smaller for athletes who move more parallel to the bar.

Table 7. Step-to-bar angle between toe-off to toe-off of each respective foot contact along with the percentage change in these angles from one to the next (1-3 indicates the % change from the first to the final angle).

Athlete	SB angle 1-2 nd TO (°)	SB angle 2-3 rd TO (°)	SB angle 3 rd -4 th TO (°)	Δ 1-2 (%)	Δ 2-3 (%)	Δ 1-3 (%)
BARSHIM	70.10	60.36	41.92	-13.89	-30.55	-40.20
LYSENKO	66.25	49.38	42.59	-25.46	-13.75	-35.71
GHAZAL	64.36	56.52	42.16	-12.18	-25.41	-34.49
RIVERA	65.24	55.76	25.91	-14.53	-53.53	-60.29
PRZYBYLKO	-	47.73	22.75	-	-52.34	-
GRABARZ	67.88	53.08	24.33	-54.16	-64.16	-54.16
IVANYUK	55.24	44.82	29.60	-33.96	-46.42	-33.96
MCBRIDE	59.02	45.39	28.69	-36.79	-51.39	-36.79
BONDARENKO	-	55.03	28.05	-	-49.04	-
ONNEN	75.13	61.46	29.13	-18.20	-52.60	-61.23

Note: Certain values could not be computed for Przybylko and Bondarenko.

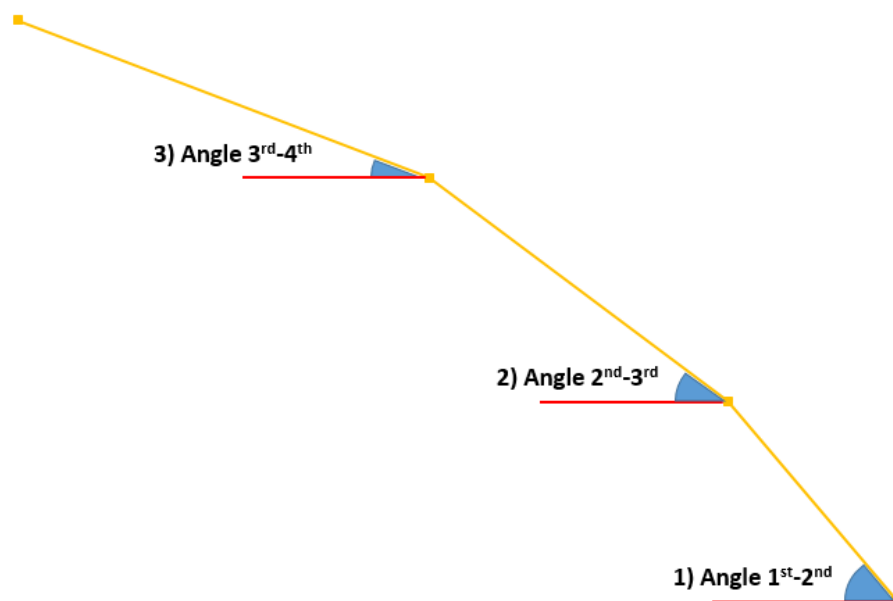


Figure 13. Schematic representation of the step-to-bar angle for each foot contact relative to the next.

Figure 14 below shows an overhead view of the CM path during the approach for each of the finalists relative to the bar (black solid line). Note: 'Right / left footers' are those who took off on the right and left legs, respectively.

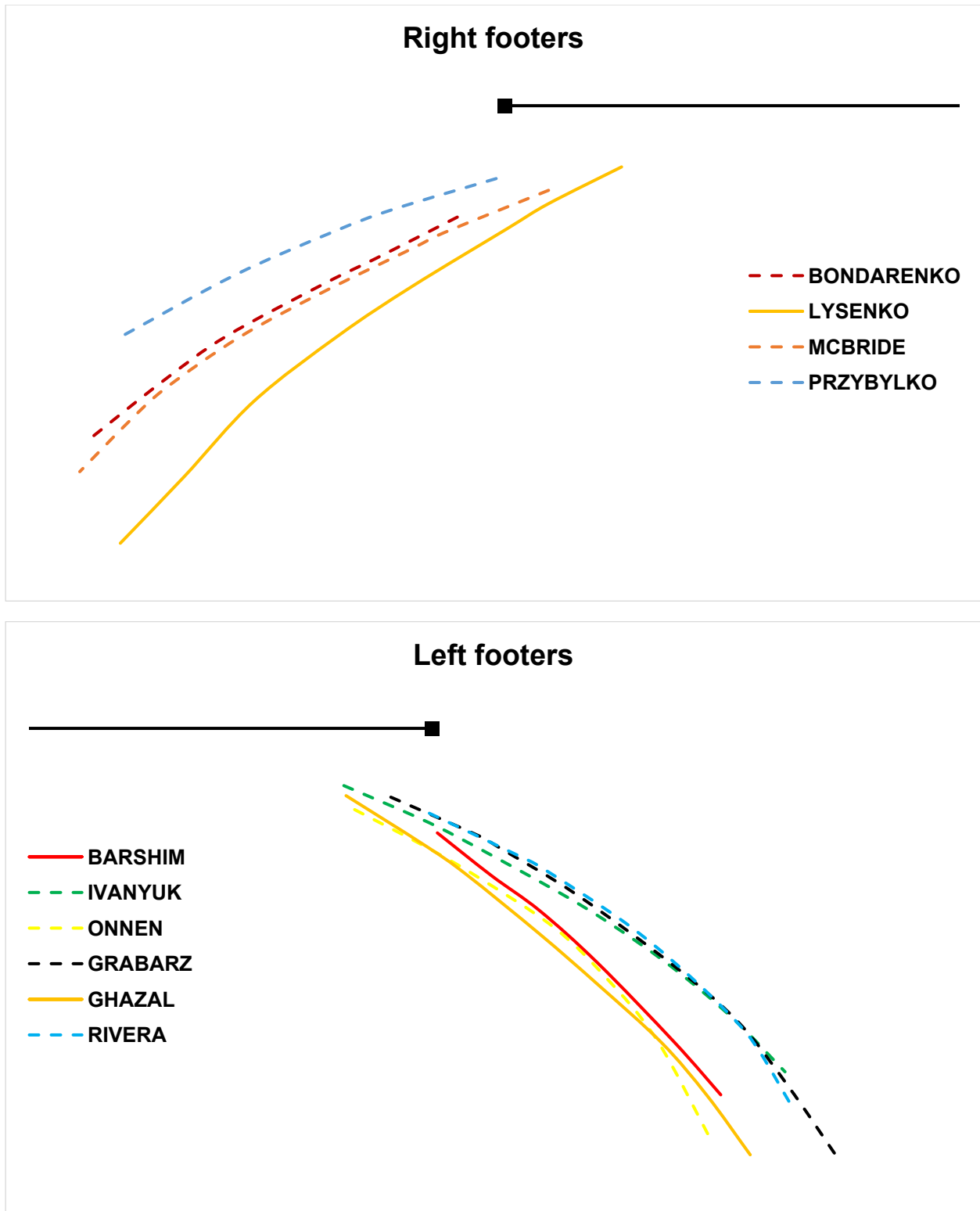


Figure 14. The overhead views of the paths of the CM during the approach and take-off for the finalists. Medallists are represented by solid lines.

Figure 15 below shows an overhead view of the whole body and foot paths during the approach, take-off and airborne phases for the three medallists.

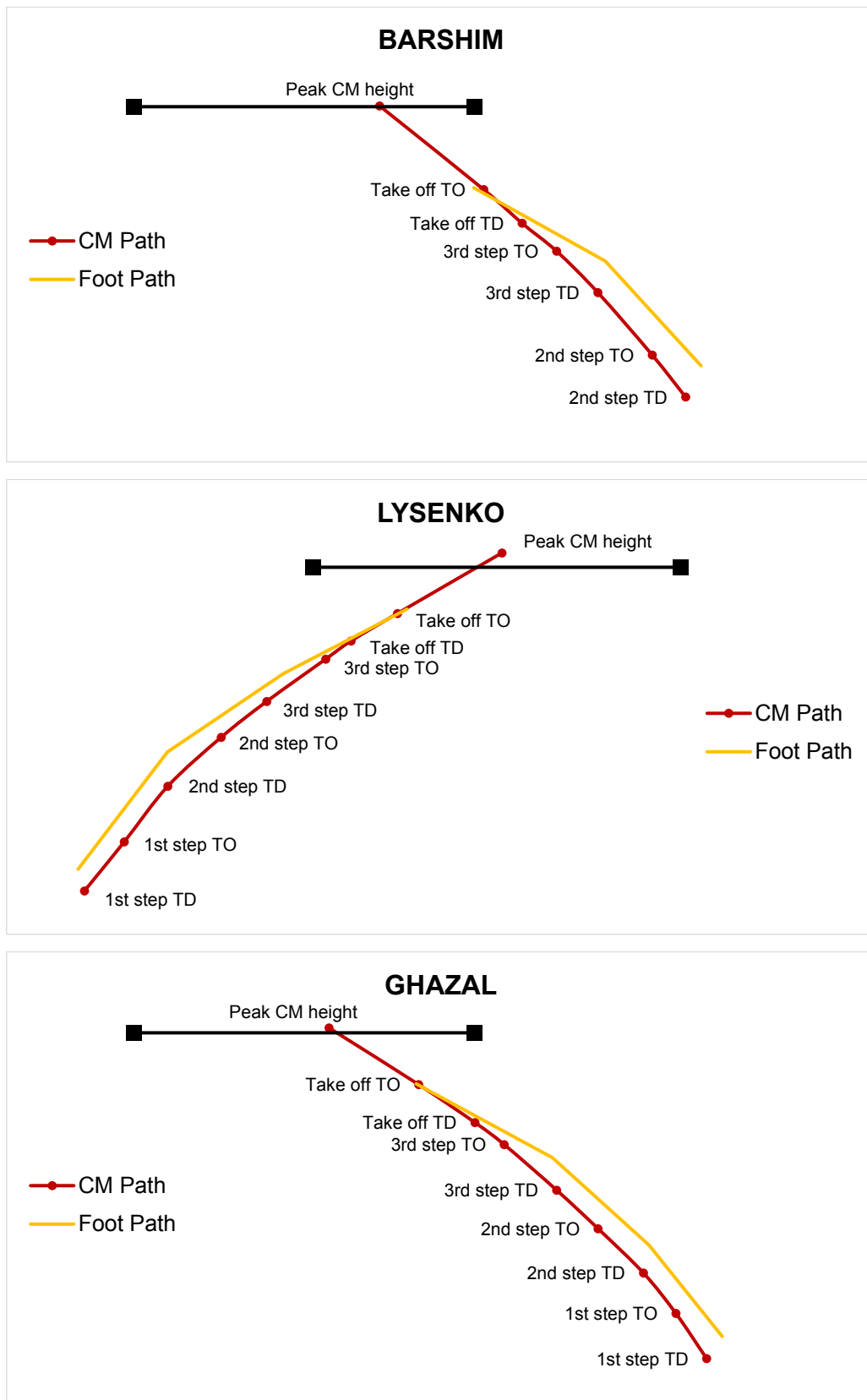


Figure 15. Overhead views of the CM and foot path during the approach, take-off and airborne phases for the three medallists.

Table 8 and Figure 16 below show the length of the last three approach steps along with the percentage change in absolute step length values (from step one to three) and duration of take-off for each of the finalists.

Table 8. The length of the last three approach steps along with the contact time of the take-off phase (CT) for the finalists. Step lengths are also expressed as a percentage of each athlete's standing height.

Athlete	1 st step (m)	2 nd step (m)	3 rd step (m)	1 st step (%)	2 nd step (%)	3 rd step (%)	Δ 3-1 %	Take-off CT (s)
BARSHIM	1.93	2.34	2.14	100.37	121.95	111.49	10.88	0.14
LYSENKO	2.67	2.14	2.03	138.85	111.36	105.68	-23.97	0.17
GHAZAL	2.05	2.12	2.22	106.44	109.59	115.18	8.29	0.19
RIVERA	1.71	1.91	1.96	89.49	99.94	102.44	14.62	0.19
PRZYBYLKO	-	2.39	2.18	-	123.30	112.12	-	0.16
GRABARZ	2.36	2.53	1.90	122.96	109.59	99.11	-19.49	0.18
IVANYUK	2.01	1.80	1.94	109.82	98.15	105.89	-3.48	0.16
MCBRIDE	1.72	1.87	1.98	91.33	99.30	105.50	15.12	0.18
BONDARENKO	-	2.11	2.18	-	106.78	110.89	-	0.16
ONNEN	2.70	2.19	2.10	139.36	112.95	108.45	-22.22	0.16

Note: Certain values could not be computed for Przybylko and Bondarenko.

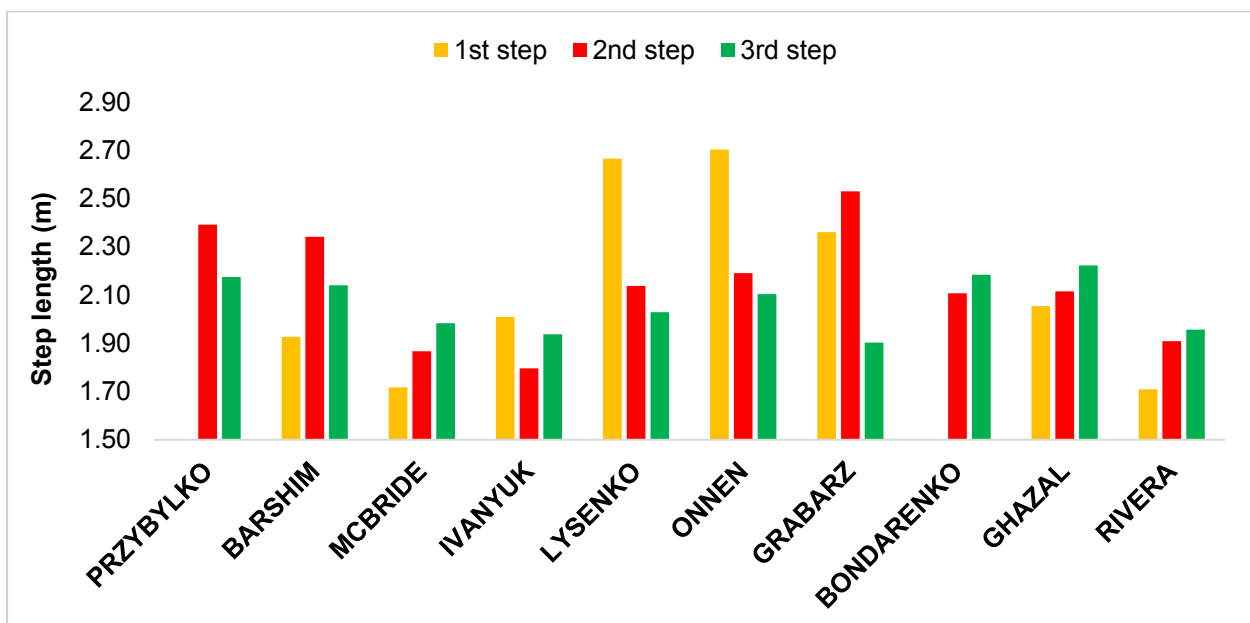


Figure 16. Length of the last three approach steps for each of the finalists.

Table 9 below shows the vertical and resultant velocities of the CM at key points during the take-off phase for each of the finalists along with various metrics showing the change in horizontal and vertical velocities with respect to each other. The take-off angle and take-off distance are also presented in the table with Figure 17 visually depicting the contrasting take-off distances adopted by two finalists.

Table 9. The vertical (V_v) and resultant (V_r) velocity values at TD and TO during the take-off phase along with the velocity transfer, take-off angle and take-off distances.

Athlete	V_v take-off TD (m/s)	V_v take-off TO (m/s)	V_r take-off TO (m/s)	Velocity transfer (%)	Δ Ratio (V_v/V_h)	Take-off angle ($^\circ$)	Take-off distance (m)
BARSHIM	-0.50	4.82	6.66	71.31	-1.85	46	1.58
LYSENKO	-0.70	4.76	5.98	77.45	-1.59	53	0.85
GHAZAL	-0.90	4.56	6.09	76.15	-1.74	49	1.03
RIVERA	-0.25	4.71	5.87	68.98	-1.35	53	1.36
PRZYBYLKO	-0.44	4.68	6.79	64.24	-1.68	44	1.08
GRABARZ	-0.76	4.52	5.93	73.74	-1.59	50	1.04
IVANYUK	-0.60	4.66	6.20	74.50	-1.77	49	0.78
MCBRIDE	-0.59	4.70	6.26	67.56	-1.43	49	1.35
BONDARENKO	-0.37	4.98	6.77	68.07	-1.57	46	1.70
ONNEN	-0.26	4.61	6.11	65.72	-1.43	49	1.22

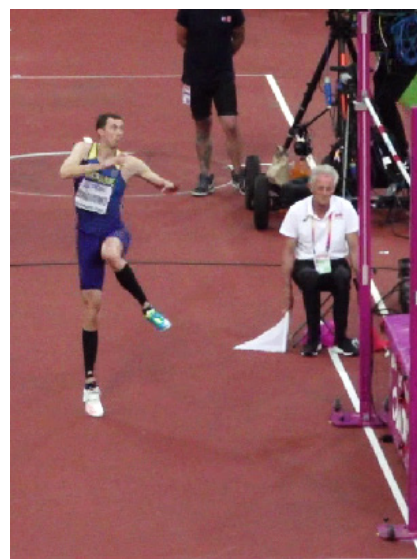
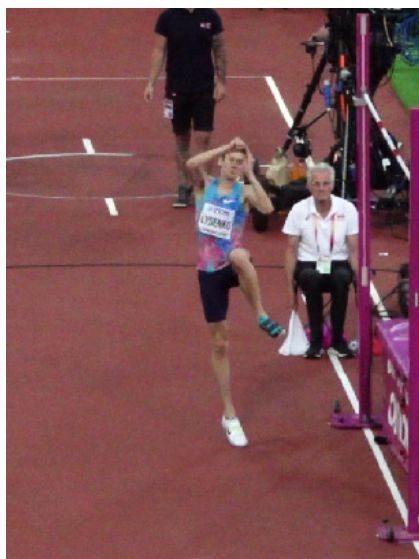


Figure 17. The contrasting take-off distances of Lysenko (left) and Bondarenko (right).

Figure 18 below shows some relationships between key variables.

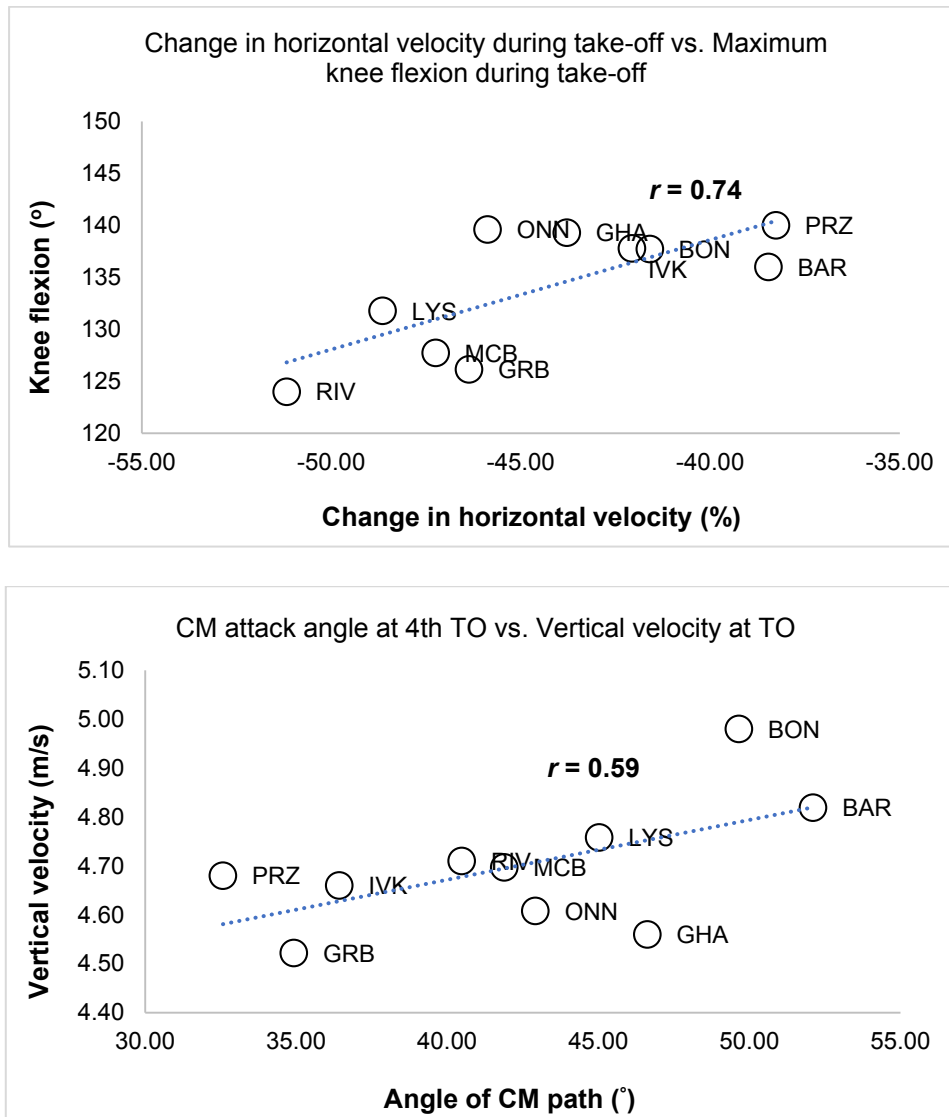


Figure 18. Scatterplots showing the relationships between key variables. r values indicate correlation coefficients.

Table 10 below shows the angles of the knee and ankle during the penultimate and final (take-off) foot contacts for each of the finalists.

Table 10. The knee angles at the instant of touchdown (TD) and toe-off (TO) during the penultimate foot contact for all finalists. Knee and ankle angles are also displayed at TD, TO and its lowest value during the final (take-off) contact.

Athlete	Penultimate				Take-off			
	Knee angle TD (°)	Knee angle TO (°)	Knee TD (°)	Knee lowest (°)	Knee TO (°)	Ankle TD (°)	Ankle lowest (°)	Ankle TO (°)
	BARSHIM	131	143	163	136	175	128	102
LYSENKO	130	138	161	132	172	127	106	137
GHAZAL	153	142	166	139	170	113	98	155
RIVERA	137	132	166	124	168	123	89	125
PRZYBYLKO	126	147	170	140	167	130	111	134
GRABARZ	155	134	169	126	173	120	92	133
IVANYUK	139	132	168	138	171	122	108	137
MCBRIDE	114	132	165	128	171	126	111	139
BONDARENKO	128	146	169	138	171	130	119	140
ONNEN	148	155	165	140	178	122	93	143

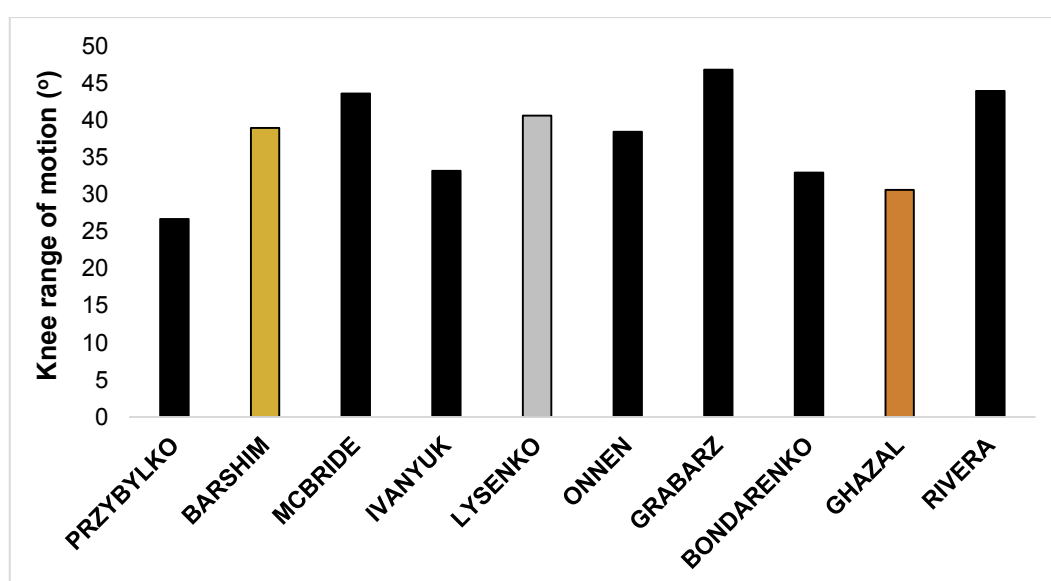


Figure 19. The range of motion of the knee (take-off leg) between maximum flexion and take-off for each of the finalists. The medallists have been highlighted in their respective medial colours whilst the remaining finalists are displayed in black.

Figure 20 below provides an indication of the contact times and flight times for the final three approach steps. Note: contact 4 represents the duration of the take-off contact.

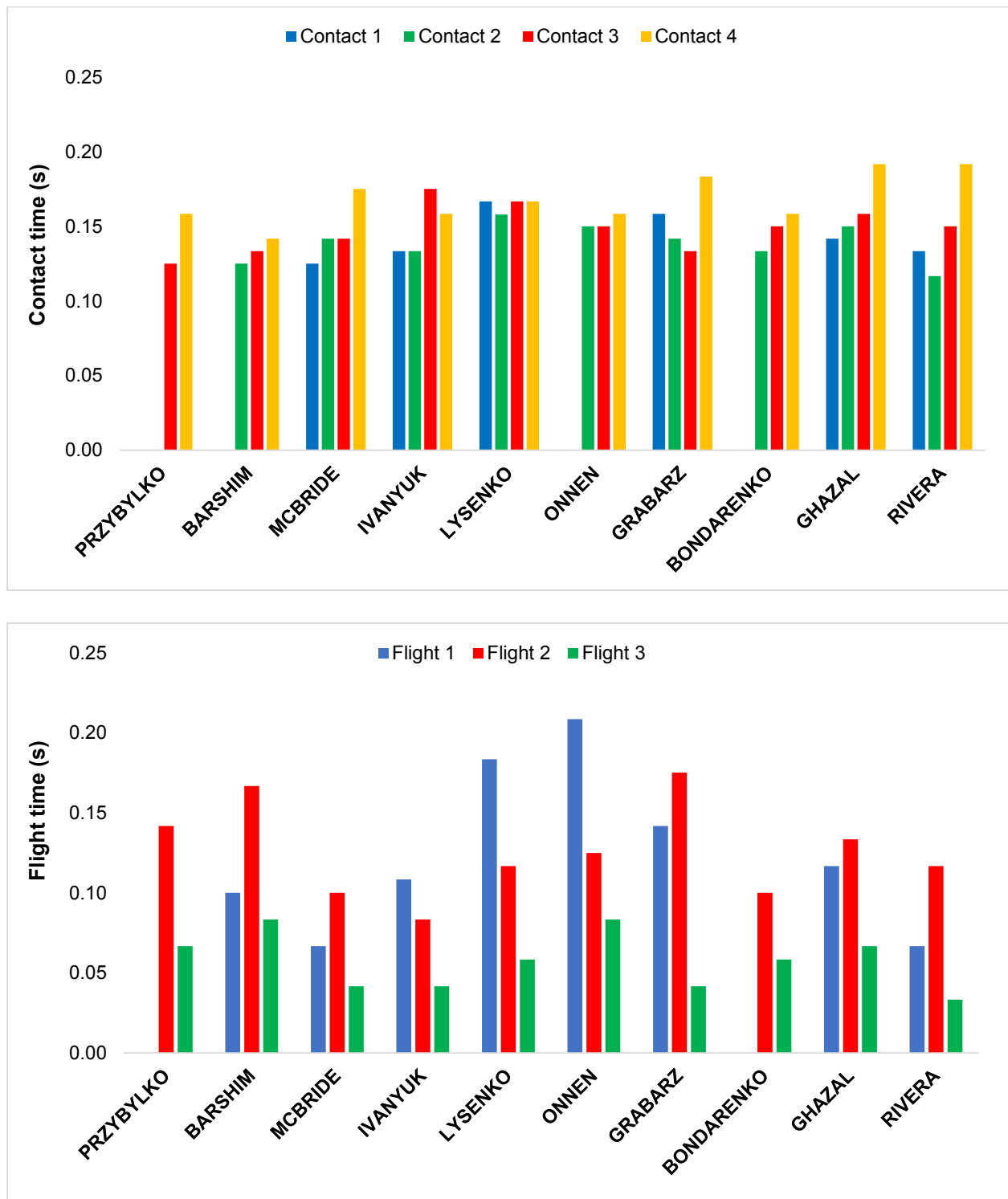


Figure 20. Top: Contact times for the final four ground contacts during the approach for each of the finalists. Bottom: Flight times for the final three steps before take-off (flight 3 precedes contact 4) for each of the finalists.

Figure 21 below shows (top) the ratio of flight time to contact time (flight time divided by the subsequent contact time) during the final step along with (bottom) the relationship between this ratio and the knee angle at maximum flexion during the take-off phase.

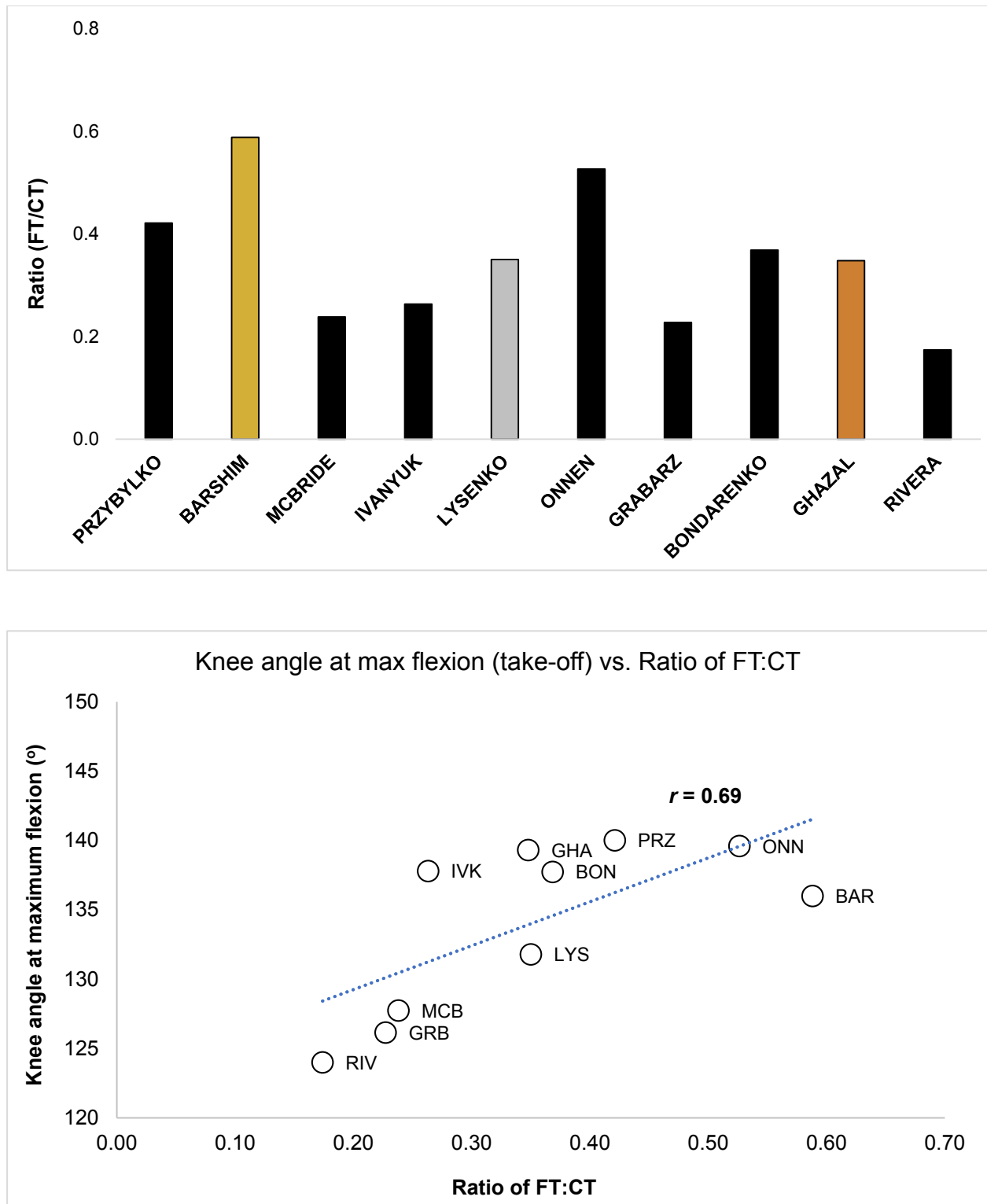


Figure 21. Top: Ratio of flight time to ground contact time during the final step. Bottom: relationship between the ratio and knee angle at maximum flexion during the take-off phase.

Table 11 and Figure 22 below show the time spent in knee flexion and extension during the penultimate and final foot contacts.

Table 11. The time spent in knee flexion and extension during the penultimate and final foot contacts.

Athlete	Penultimate contact		Final contact	
	Flexion (s)	Extension (s)	Flexion (s)	Extension (s)
BARSHIM	0.06	0.08	0.08	0.07
LYSENKO	0.07	0.09	0.09	0.08
GHAZAL	0.09	0.07	0.13	0.06
RIVERA	0.07	0.08	0.12	0.08
PRZYBYLKO	0.01	0.12	0.10	0.06
GRABARZ	0.08	0.06	0.11	0.08
IVANYUK	0.09	0.08	0.09	0.07
MCBRIDE	0.08	0.07	0.10	0.08
BONDARENKO	0.10	0.05	0.09	0.07
ONNEN	0.08	0.08	0.08	0.08

Note: Any differences in the duration of final contact from the Table 8 are a result of rounding differences.

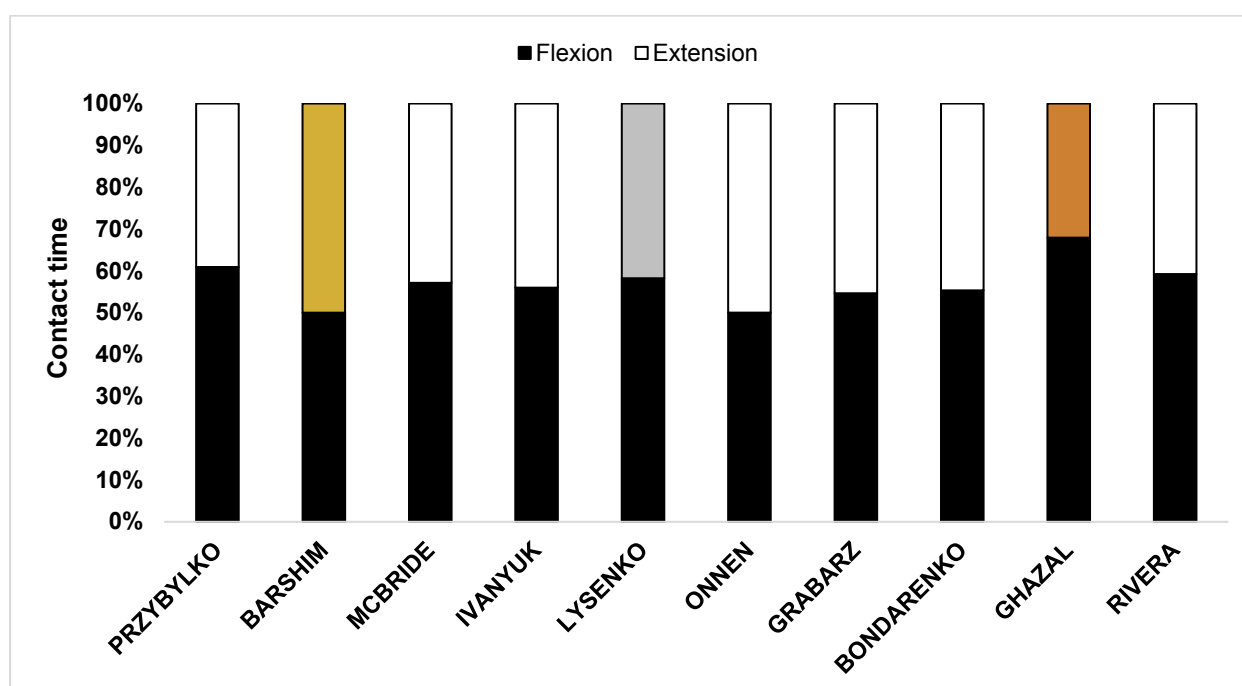


Figure 22. The percentage of time spent during knee flexion and extension during the final foot contact (take-off phase).

Table 12 below shows the whole-body and trunk lean at touchdown during the take-off phase along with the sideways lean of the trunk at TD. Figure 23 provides an example of body orientation at touchdown for one of the finalists.

Table 12. The whole-body lean at touchdown and toe-off during the take-off phase and the trunk lean at touchdown for each of the finalists.

Athlete	Whole-body lean (°)		Trunk lean at	Side-ways trunk lean at
	TD	TO *	TD (°)	TD (°)
BARSHIM	36	-1	10	6
LYSENKO	38	0	21	4
GHAZAL	40	-2	17	7
RIVERA	45	-1	22	9
PRZYBYLKO	37	-3	18	10
GRABARZ	44	-3	20	8
IVANYUK	44	0	19	5
MCBRIDE	43	-7	20	13
BONDARENKO	39	-3	17	11
ONNEN	35	-4	14	9

Note: * negative value provides an indication of forward lean.



Figure 23. Example of body orientation at TD during the take-off phase for Barshim.

COACH'S COMMENTARY

In terms of producing peak performance at the season's most important meeting only Rivera recorded a season's (outdoor) best in the final although Grabarz and Ivanov (the latter pulling out of the final through injury) recorded their season's best in the qualifying round. The other finalists recorded their season's best between twelve weeks before two weeks after the championships.

The aim in the high jump event is for the athlete is to project the entire body over an increasingly raised horizontal fibreglass lath set on two narrow pegs without dislodging it. To be successful the athlete faces several challenges:

- Create sufficient horizontal momentum to pass from one side of the bar to the other
- Maximise the conversion of horizontal to vertical momentum to raise the body high enough to clear the bar
- Adjust the body position during the flight so as not to dislodge the bar

The final part of high jump approach comprising a series of chords is commonly referred to as a "curve". Adopting this approach run pattern is designed to enable the athlete to arrive at the point of take-off with lateral and rearward displacement of the CM with respect to the final foot contact with a low centre of mass (CM) while minimising knee and hip flexion and speed loss. Such a position is intended to allow the athlete to develop necessary tri-axial angular momentum during the actual take-off.

Biomechanically the high jump is a complex event. Uniquely when compared to the other three jump events in athletics, an effective take off can be produced over a wide time frame ranging from 0.11 secs (Dmitrik in Daegu 2011) to 0.20 seconds (Moya in Helsinki 2005). In London this time frame ranged from 0.14 seconds to 0.19 seconds.

Additionally the athlete has the freedom to approach the take off point at an angle and speed of their choosing, select a take-off point relative to the bar in order to best generate the forces, vectors and rotations necessary for successful performance. There was some noted commonality. All athletes used a "curve" in the last three strides of the approach, displayed sideways lean away from the bar, had their shortest flight time between the penultimate and plant contacts (0.04 to 0.09 seconds) and employed a heel first plant. The recorded data also illustrated the great diversity in technical application between athletes.

- There was a large range final approach run angles (step-to-bar) Lysenko (42.6 degrees) to Przybylko (22.8 degrees).
- Approach run angle (step-to-bar) change during the last stride ranged from seven degrees (Lysenko) to thirty two degrees (Onnen).
- Take off distance from the bar ranged from 0.85 m (Lysenko) to 1.70 m (Bondarenko).

-
- Sideways lean at plant ranged from 4 degrees (Lysenko) to 13 degrees (McBride).
 - In the last two steps of the approach, half the athletes used a long/short pattern, half a short/long stride pattern (Table 8).
 - One stride before plant, five athletes touched down ball of foot first, one athlete used a full foot contact the remaining four used a heel contact (determined visually from video footage).
 - Eight athletes showed increased ground contact times in the final strides of the approach.
 - A variety of different arm actions were noted. One “original Fosbury” running arm action (Bondarenko), a bar side single arm lead (Onnen), with the other eight finalists all using a double arm shift with both arms being brought forward during the penultimate stride apart from Przybylko who held back his bar side arm during the penultimate stride.
 - Most athletes lowered their CM during the last step with two (Bondarenko and Onnen) raising their CM into plant (Table 4).
 - Seven athletes employed a tightly folded free knee. Only three athletes (Rivera, Grabarz and McBride) employed an “open knee” free leg swing. Interestingly these three athletes also tended to show longer time on the ground in the take-off (0.18-0.19 seconds).
 - Peak CM height location ranged from 29 centimetres beyond (Lysenko) to 23 centimetres in front of the bar (Rivera) with most jumper’s CM high point falling within 10 centimetres of the bar. Only Barshim had his high point above the bar.

While all three medalists maintained relatively high final approach (step-to-bar) angle (~42 degrees), there was a sharp contrast in styles between Barshim and Lysenko who both topped both the podium and the world rankings in 2017.

Barshim’s jump was typified by great horizontal speed. Adopting a long/short pattern in the last two strides of the approach, his last two ground contacts were very short (0.13-0.14 seconds). Of all the jumpers he displayed the highest ratio of flight time to contact time (Figure 21) and an average (39 degrees) of concentric knee motion during take-off. His gently curving approach and a high CM enabled him to run fast. He also displayed a high final (step-to-bar) angle (42 degrees) that required a distant take-off (> 1.50 m) from the bar and significant long axis rotation to place his high point above the bar. He was able to demonstrate an efficient “layout position” with his CM (2.38 m) only 3 centimetres above the bar. His final approach angle combined with his more upright trunk position at plant, low levels of sideways trunk lean (Table 12), quickness over the plant foot and a tightly folded knee assisted in maintaining a stable foot plant. Understandably with his great speed and short take-off time his final take-off angle was relatively low. This technique can be described as requiring extreme levels of elasticity.

With noticeably less speed and longer ground contacts (0.16-0.17 seconds) in the approach and at take-off, Lysenko also chose to use a gently curving approach with a high final (step-to-bar)

angle to the bar (42.6 degrees). Displaying a lower ratio of flight time to contact time than Barshim (Figure 21), the slower approach run speed and effective use of swinging limbs was reflected in his ability to efficiently convert his horizontal to vertical velocity (77% - Table 9). This enabled him to achieve a high take-off angle (53 degrees) and a high position of the CM (as a proportion of body height) at take-off.

In his penultimate stride Lysenko loaded the take-off leg with noticeable negative vertical velocity following a short flight time (0.06 seconds). Despite having a proportionately longer eccentric component during the plant contact and maximum knee flexion of 132 degrees (take-off leg) he was helped by a fast tightly folded swing leg to work concentrically through a 40 degree range, completing the take-off in 0.17 seconds which is indicative of great levels strength and power. This take-off enabled him to raise his CM to 2.40 m eight centimetres above the bar. However his high point was some 29 centimetres beyond the plane of the bar. At critical heights he may be advised to adopt a more distant take-off position than his recorded 0.85 m in order to consistently position his CM above the bar and lessen the risk of hitting and dislodging the bar from the pegs.

It was noted that the three medallists all had high final angles (step-to-bar) of approach and only made small angle changes towards the end of the approach. These may be characteristics worth adopting. With the reported changes in whole body lean (inward and backwards) and the small degrees of inward lean (Table 11), when developing technique, coaches may wish to consider the ratio between transverse and frontal axes rotation during take-off.

At take-off Lysenko's lateral lean was minimal (4 degrees) but he possessed noticeable whole body and trunk lean (Table 12). This may have contributed to his ability to maintain excellent foot stability with no evident pronation. To harness and maximise the generation and transmission of forces during the take-off, joint stiffness and stability in the take-off leg at both knee and ankle is desirable. In this regard over pronation in the plant is undesirable. In the men's final 50% of the finalists displayed over pronation at take-off (determined visually from high-speed video footage). Four of these (Ghazal, Rivera, Grabarz and Onnen), also had the greatest degree of ankle flexion, with Rivera, Grabarz and Onnen also making a large (30 degrees) change in direction in the penultimate contact leading to a relatively narrow final angle to the bar (24-29 degrees). Ghazal, Rivera and Grabarz also recorded a long eccentric phase (0.11-0.13 seconds) in the take-off contact and spent the longest time on the ground in the take-off (0.18-0.19 seconds).

In Ghazal's case, a short / long stride pattern, the largest amount of negative vertical velocity into plant, deep ankle flexion and a long eccentric phase (in both the penultimate and particularly plant contacts) may have been the cause of his over pronation given his small angle changes at the end of the approach. Przybylko with an extremely fast approach, a large change of direction in the last stride (25 degrees), a wide final approach angle (22.8 degrees) and a relatively long

eccentric at component at plant (although notably short in the penultimate contact) also displayed pronation. Minimising pronation at take-off is important to allow effective force transmission and to prevent overstress to the soft tissues of the lower limb. Coaches may wish to consider the potential effects of the above combination of factors (particularly the amount of angle change per step, sideways lean and final direction into plant) when building a technical model.

Interesting trends can be seen in some of the relationship data such as the positive correlation between leg stiffness and the ability to reduce knee flexion (Figure 21). While certain factors such as the ability to development vertical momentum are critical to the performance of the event, the fact that the gold and silver medallists utilise greatly differing techniques confirm the fact, noted in previous studies, that it is possible to adopt a variety of technical interpretations and still be successful. The challenge for the coach is to develop the technique that best suits the physical makeup of their athlete.

CONTRIBUTORS

Dr Gareth Nicholson is a Senior Lecturer in Sport and Exercise Biomechanics at Leeds Beckett University and is Course Leader for the MSc Sport & Exercise Biomechanics pathway. Gareth has First Class Honours in BSc Sport and Exercise Science as well as an MSc in Sport & Exercise Science and a PhD from Leeds Beckett University. Gareth's research interests are in the measurement and development of strength and power. Gareth currently supervises a range of health and performance-related research projects.



Dr Athanassios Bissas is the Head of the Biomechanics Department in the Carnegie School of Sport at Leeds Beckett University. His research includes a range of topics but his main expertise is in the areas of biomechanics of sprint running, neuromuscular adaptations to resistance training, and measurement and evaluation of strength and power. Dr Bissas has supervised a vast range of research projects whilst having a number of successful completions at PhD level. Together with his team he has produced over 100 research outputs and he is actively involved in research projects with institutions across Europe.



A retired Head of Physical Education, Denis Doyle is an IAAF Level Five Elite Jumps coach and holds UKA Level Four Performance Coach. He has coached for 49 years across all sectors of the sport and has experience as a team manager for Great Britain and England and as a coach with British, Irish and Indian teams at four Olympics and six World Championships. His personal coaching record includes guiding over thirty five athletes from several nations to international success, five at Olympic level, with ten of them setting national senior and age group records. He is currently coach to 2nd world ranked U20 high jumper Tom Gale.

